

# Studies with Lysine N<sup>6</sup>-Hydroxylase. Effect of a Mutation in the Assumed FAD Binding Site on Coenzyme Affinities and on Lysine Hydroxylating Activity

Matthias Stehr<sup>1</sup>, Liliana Smau<sup>2</sup>, Mahavir Singh<sup>3</sup>, Oliver Seth<sup>2</sup>, Peter Macheroux<sup>4</sup>, Sandro Ghisla<sup>2,\*</sup> and Hans Diekmann<sup>1</sup>

<sup>1</sup> Institut für Mikrobiologie, Universität Hannover, Schneiderberg 50, D-30167 Hannover, Germany

<sup>2</sup> Universität Konstanz, Fakultät für Biologie, Postfach 5560 M644, D-78457 Konstanz, Germany

<sup>3</sup> GBF-Gesellschaft für Biotechnologische Forschung mbH, Mascheroder Weg 1, D-38124 Braunschweig, Germany

<sup>4</sup> Institut für Pflanzenwissenschaften, ETH-Zürich, Universitätstr. 2, CH-8092 Zürich, Switzerland

\* Corresponding author

The proposed FAD binding site of L-lysine N<sup>6</sup>-hydroxylase (EC 1.14.13.99) exhibits an unusual proline in a position where a highly conserved glycine is found in other FAD dependent hydroxylases. We have studied the role of this proline by mutating it to glycine in [P14G]*aerA*, which was expressed in *Escherichia coli* M15-2 and purified to homogeneity. The mutation has marked effects on the affinities of the cofactors FAD and NADPH as well as the substrate, lysine. Compared to the wild-type enzyme, the activity vs. pH profile of the mutant protein indicates a shift of the apparent pK<sub>s</sub>'s (7.8 and 8.7 for wild-type and 6.8 and 7.7 for the P14G-mutant enzyme) and of the activity maximum (pH 8 for wild-type and pH 7 for the P14G-mutant enzyme). While the activity of the mutant enzyme is much lower under conditions found to be optimal for the wild-type enzyme, adjustment of substrate and cofactor concentrations and pH leads to comparable activities for the mutant enzyme. These results suggest that the proline fulfils an important structural role in the proposed FAD binding site.

**Key words:** Aerobactin / Enzyme kinetics / Flavoprotein in monooxygenase / Lysine / Nucleotide binding / Site-directed mutagenesis.

## Introduction

Lysine N<sup>6</sup>-hydroxylase, the first enzyme in the biosynthesis of the siderophore aerobactin (Braun, 1981), catalyzes the hydroxylation of the terminal amino group of L-lysine to N<sup>6</sup>-hydroxylysine. The gene for this enzyme is part of the aerobactin operon, located on the virulence plasmids

pColV-K311, designated as *aerA* (Gross *et al.*, 1985) and pColV-K30, designated as *iucD* (de Lorenzo *et al.*, 1986). Aerobactin has been shown to be a virulence factor for pathogenic *Escherichia coli* strains and other members of the Enterobacteriaceae (Weinberg, 1984). The enzymatic reaction depends on NADPH and FAD and consumes molecular oxygen which classifies the enzyme as an external flavoprotein monooxygenase with properties similar to flavoprotein monooxygenases of the EC group 1.14.13 (Plattner *et al.*, 1989). Most of these enzymes have a conserved amino acid motif for FAD binding consisting of the sequence Gly-X-Gly-X-X-Gly located near the N-terminus of an  $\alpha$ -helix (Wierenga *et al.*, 1985). We have recently emphasized that all known N-hydroxylating enzymes involved in siderophore biosynthesis carry a proline instead of the last glycine in this nucleotide fingerprint motif (Stehr *et al.*, 1998). This observation raises the question whether this unusual replacement has any effect on FAD binding to lysine N<sup>6</sup>-hydroxylase (LH). The weak binding of FAD to the wild-type (wt) enzyme ( $K_d = 30 \mu\text{M}$ ) reported earlier (Macheroux *et al.*, 1993) has provoked us to speculate that the glycine to proline exchange in the N-terminal nucleotide binding fold is involved in causing the high dissociation constant. To investigate the importance of this proline, we have introduced a mutation in *aerA* in an attempt to restore a typical nucleotide binding site.

Here we report the kinetic properties of P14G-LH in comparison with the wt-LH. In order to improve and facilitate protein expression and purification we have also developed a new expression system of the enzyme: the complete lysine N<sup>6</sup>-hydroxylase gene (*aerA*) from the pBR322 derived vector pRG111 (Engelbrecht and Braun, 1986) was inserted into pQE30 (Figure 1A) resulting in pMR30 (Hermes *et al.*, 1994). While the enzyme was expressed from pRG111 under iron deprivation, lysine N<sup>6</sup>-hydroxylase on pMR30 is expressed as an N-terminal His-tag fusion protein under the strong *lac* promoter of pQE30. The *aerA* gene in pMR30 was then subjected to site-directed mutagenesis and the mutant protein expressed and purified as described below.

## Results

### Nucleotide-Sequence of *aerA*

The mutation [P14G] was confirmed by sequencing the [P14G]*aerA* gene. Sequencing of the entire gene (see Materials and Methods) showed that, except for the mutation introduced by site-directed mutagenesis, [P14G]*aerA*

was identical to the template *aerA*. The sequence is, however, different from that of the published sequence *iucD* (Herrero *et al.*, 1988). It should be noted that the nucleotide sequence of *iucD* was derived from pColV-K30 (Herrero *et al.*, 1988), and the *aerA* gene in pMR30 was obtained from pColV-K311 (Gross *et al.*, 1984). The differences are shown in Table 1. In the DNA sequence of *aerA*, we found the triplets for only 5 cysteines compared to six in the published sequence of *iucD* (Herrero *et al.*, 1988). This is in agreement with DTNB [5,5'-dithiobis-(2-nitrobenzoic acid)]-titration studies in the presence of the denaturant SDS (0.2%) where only five cysteine residues could be detected (Koch, M., Macheroux, P., and Ghisla, S., unpublished).

### Construction of the [P14G]*aerA* Gene and Expression of P14G Lysine Hydroxylase

For site-directed mutagenesis, the triplet CCA for Pro-14 in *aerA* was replaced by the triplet GTT coding for Gly (Figure 1B). A 77 bp primer which contained the mismatched triplet (GGT), the recognition sequence for *Bam*HI and for the enterokinase-cleaving site, was used as the forward primer. The reverse primer (27 bp) contained parts of the sequence of *aerA* and pQE30 and also the *Pst*I cleaving site. The length of the PCR fragment was estimated by agarose gel electrophoresis and the  $\approx$  1300 base pair fragment was purified and cloned in pQE30 (Figure 1B).

Seven out of 8 tested clones in *E. coli* M15 expressed a 51 kDa protein, suggesting the presence of a [P14G]*aerA*. One transformant, showing identical sequence with the template DNA, only carrying the CCA $\rightarrow$ GGT substitution was designated *E. coli* M15-2 and used for further experiments.

When strain M15-2 was grown in the fermenter under the same conditions as strain M15-0 the mutant enzyme was obtained as inclusion bodies. Soluble protein was only obtained upon growth of M15-2 at 30 °C and induction with 0.1 mM IPTG at an  $OD_{578} = 1$ . Harvesting and purification of P14G lysine hydroxylase was performed as described in Materials and Methods. This yields an apparently pure protein, which migrates as a single band on SDS PAGE (Figure 2) and a molecular mass identical to that of wt-LH. The total activity obtained is 5 U from 10 g of cells (wet weight), which is about 20% of the activity of the fully induced wt-LH when measured under the same conditions.

**Table 1** Differences between the Sequences Determined from *aerA* (pColV-K311) (Gross *et al.*, 1985; this work) and *iucD* (pColV-K30) (Herrero *et al.*, 1988).

AA position	<i>iucD</i> (pColV-K30)	<i>aerA</i> (pColV-K311)
139	CAA (Gln)	GAA (Glu)
172	AGT (Ser)	ATG (Met)
178	GAT (Asp)	GAC (Asp)
214	GTG (Val)	GTC (Val)
231	GAT (Asp)	GAG (Glu)

AA, Amino acid; Ser, serine; Met, methionine; Asp, aspartic acid; Val, valine; Glu, glutamic acid.

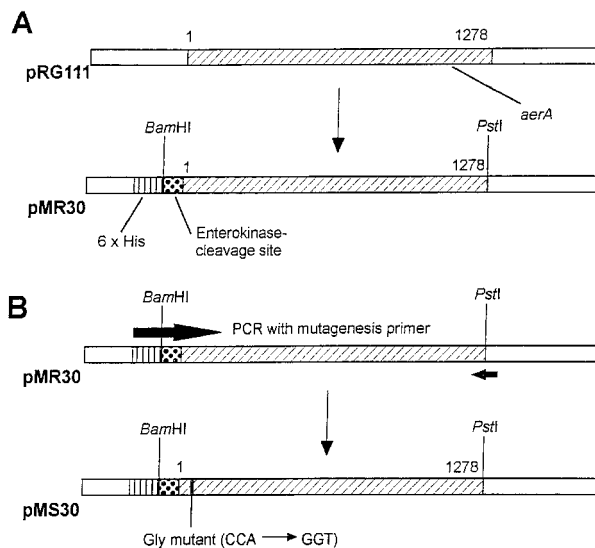


**Fig. 1** Schematic Representation of the Construction of *aerA* Clones Used in This Study.

(A) Construction of pMR30. The DNA fragments from pRG111 and pMR30 are indicated by white boxes. Hatched lines represent the coding region for lysine N<sup>6</sup>-hydroxylase of *E. coli* (*aerA*). Boxes coding for the PCR-introduced enterokinase site and the His-tag are marked.

(B) Site directed mutagenesis of *aerA* resulting in [P14G]*aerA* and construction of pMS30. The Pro-14 (CCA) residue was replaced with Gly (GGT) by PCR using a mutagenesis primer (indicated by large arrow).

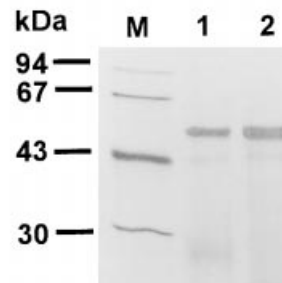


**Fig. 2** SDS-PAGE Gel of Purified P14G-LH and Comparison with wt-LH.

Lane 1, wt-LH; lane 2, P14G-LH (51 kDa); M, marker. The purification was carried out by Ni-NTA affinity chromatography as detailed in the Materials and Methods section. SDS-12% PAGE was performed as described by Laemmli and Favre (1973) and proteins were visualized by silver staining (Blum *et al.*, 1988).

### Partial Kinetic Characterization of the P14G Mutant Protein

When P14G-LH was first analyzed under experimental conditions described to be optimal for wild-type lysine N<sup>6</sup>-hydroxylase, the observed activity, both in terms of L-lysine hydroxylating and NADPH-oxidase activity, was greatly reduced suggesting that the proline to glycine exchange has severely compromised the catalytic efficiency of the P14G-LH. However, when the experimental conditions, such as FAD, NADPH and L-lysine concentration as

well as the pH, were optimized for P14G-LH comparable activities were observed.

Figure 3 shows the activity of wild-type and P14G-LH, measured with the NADPH assay, as a function of the FAD concentration. With wt-LH, surprisingly, a cofactor inhibition at very high FAD concentrations is apparent, which is also influenced by the concentration of L-lysine. The dependence can be satisfactorily fitted with a typical equation for simple inhibition by a reactant (see Materials and methods for details; Fersht, 1977, pp. 98, equation 3.51). Thus, under these conditions the apparent  $K_m$  for the activity increase is  $\approx 10$  and  $\approx 4 \mu\text{M}$  at 0.3 and 1.5 mM [L-lysine] respectively, and the apparent  $K_i$  for FAD is of the order of 2 and 1 mM, respectively. With P14G-LH, the data points can be fitted either using the classic Michaelis-Menten relationship ( $R^2 = 0.95$ ), or, marginally better, with the same equation describing substrate inhibition as for wt-LH ( $R^2 = 0.97$ ). From preliminary measurements at  $[\text{FAD}] > 300 \mu\text{M}$  (not shown) it is clear that cofactor inhibition also occurs with P14G-LH at high concentrations of FAD. The  $K_m$  of FAD for P14G-LH can be estimated as  $\approx 400 \pm 40 \mu\text{M}$  (Figure 3). Based on the fact that LH interacts with the two nucleotides FAD and NADPH/NADP<sup>+</sup> with  $K_m$  values of similar magnitude, it is assumed that each of these two cofactors can interfere with the binding of the other at high concentrations.

A similar behaviour was found for the activity dependence on the NADPH concentration as shown in Figure 4.

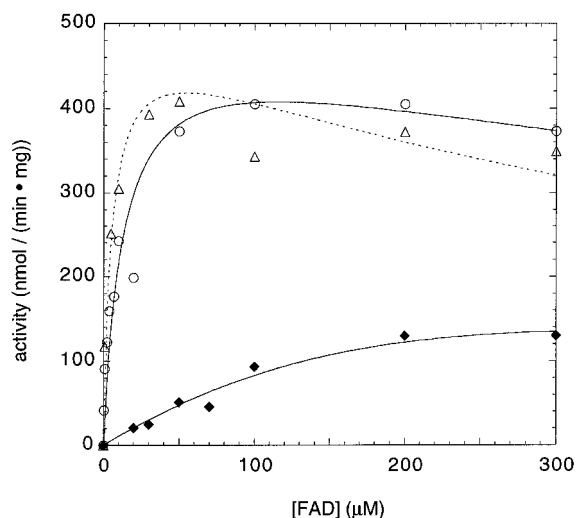


**Fig. 3** Dependence of the Specific Activity of LH from the FAD Concentration.

Activity measurements were performed as detailed in the Materials and Methods section (see NADPH oxidation assay) and in the presence of  $300 \mu\text{M}$  NADPH. (○): wt-LH in the presence of  $300 \mu\text{M}$  and (△): of 1.5 mM L-lysine. (◆): P14G-LH in the presence of 1.5 mM L-lysine. The traces for wt-LH were obtained using the equation described for substrate inhibition (Fersht, 1977, pp. 98, equation 3.51) and, for (△):  $K_m \approx 4 \mu\text{M}$ ,  $K_i \approx 1 \text{ mM}$  and maximal activity = 450 [nmol/(min × mg)], respectively for (○):  $K_m \approx 10 \mu\text{M}$ ,  $K_i \approx 2 \text{ mM}$  and maximal activity = 450 [nmol/(min × mg)]. The trace for P14G-LH (◆) was obtained using the same equation as for wt-LH and the resulting  $K_m$  was about  $400 \mu\text{M}$  ( $K_i \approx 300 \mu\text{M}$ ). See text for further details.

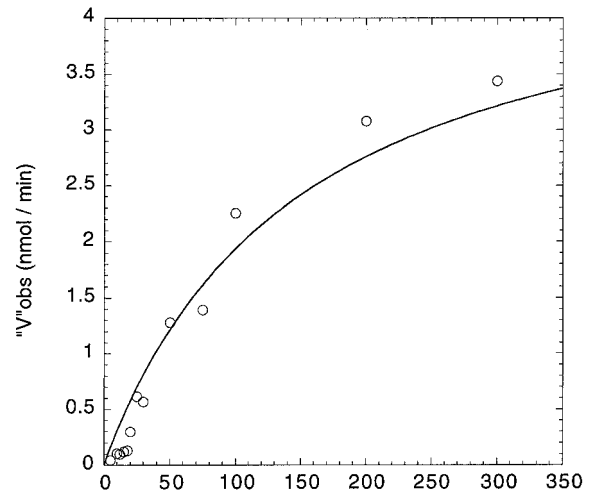


**Fig. 4** Dependence of the Specific Activity of LH from the NADPH Concentration.

The (○) data points were obtained in the presence of 1.5 mM L-lysine and  $300 \mu\text{M}$  FAD. The curve was obtained using the Michaelis-Menten equation and  $K_m = 150 \mu\text{M}$ , ' $v_{\text{obs}}$ ' = 4.8 (nmol/min). See text for further details.

In contrast to the case with FAD, however, the onset of activity can be fitted with reasonable results to a curve based on the Michaelis-Menten equation, yielding a  $K_m \approx 150 \mu\text{M}$ . At concentrations of NADPH  $> 300 \mu\text{M}$  the activity rapidly decreases (not shown). With P14G-LH the rate of NADPH oxidation is increased approx. three-fold at saturating [L-lysine], as compared to the rate in the absence of lysine (Table 2B). With wt-LH the corresponding increase

**Table 2** Activity of the P14G Lysine N<sup>6</sup>-Hydroxylase in Iodine- and NADPH-Oxidation Assays.

A) Iodine-oxidation assay

Enzyme	[enzyme] (mg/ml)	[FAD] ( $\mu\text{M}$ )	mU (nmol/min)	Specific activity (nmol/(min × mg))
P14G mutant	0.1	5	0.12	1.1
	0.05	300	1.54	28
Wild-type LH	0.01	5	1.02	300

B) NADPH-oxidation assay

Enzyme	[enzyme] (mg/ml)	[FAD] ( $\mu\text{M}$ )	$\Delta\text{OD}/\text{min}$	mU (nmol/min)	Specific activity [nmol/(min × mg)]
P14G-mutant	0.025	5	0.001	0.16	5.82
		300	0.024	3.85	140
		0.0075*	1.2*	43.6*	
Wild-type LH	0.025	10	0.07	11.1	444

\* assayed in the absence of L-lysine.

is  $\approx 10$  fold (Macheroux *et al.*, 1993). The activity measured with the NADPH-oxidation test is comparable for wt-LH and P14G-LH under conditions optimized for the two proteins (at 5 and 300  $\mu\text{M}$  FAD, respectively and at different pH values as shown in Figure 6, below). In contrast to this, with the iodine-oxidation test a 10-fold smaller activity for P14G-LH was found (Table 2A). This indicates a higher extent of uncoupling of lysine hydroxylation from NADPH oxidation. Thus, with the mutant protein production of N-hydroxylated lysine is only  $\approx 10\%$  compared to NADPH-oxidation under these conditions.

With respect to changes of the L-lysine concentration, the behavior of P14G-LH is also significantly different compared to wt-LH. For the latter, substrate inhibition has been reported (Macheroux *et al.*, 1993). In contrast, the P14G-LH activity increases asymptotically as shown in Figure 5. However, this approach to saturation is biphasic as demonstrated also by the double reciprocal plot (Figure 5, inset). This behavior is symptomatic of two binding modes. The increase of activity at low concentrations of L-lysine proceeds with  $K_{m1} \approx 8 \mu\text{M}$ , which is approx. 15-fold lower than that reported earlier for the wild-type enzyme (Macheroux *et al.*, 1993). At higher concentrations of L-lysine a second phase of saturation can be deduced which reflects  $K_{m2} \approx 5 \text{ mM}$ ; this is some 40-fold higher than that observed with wt-LH.

A major difference between mutant and wt-LH is observed in the pH dependence of the activity, as depicted in Figure 6, where the data reported by Macheroux *et al.* (1993) for wt-LH are included for the purpose of comparison. This graph shows that maximum attainable activity is

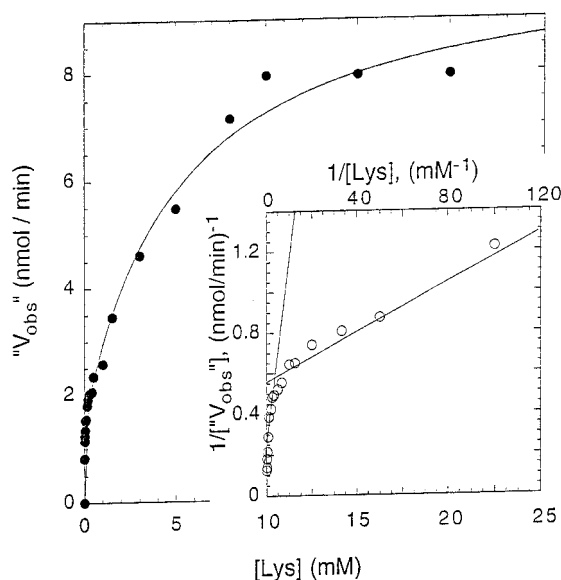


**Fig. 5** Dependence of the Specific Activity of LH from the L-Lysine Concentration.

Experimental conditions: [FAD] and [NADPH] = 300  $\mu\text{M}$ . The fit to the (●) data points was obtained using a Michaelis-Menten equation adapted for two substrate binding modi and using  $V_{max1} = 1.5$  (nmol/min),  $V_{max2} = 8.6$  (nmol/min),  $K_{m1} = 8 \mu\text{M}$  and  $K_{m2} = 5 \text{ mM}$ . Inset (○): double reciprocal plot of the initial rates of NADPH-oxidation versus the L-lysine concentration. See text for further details.

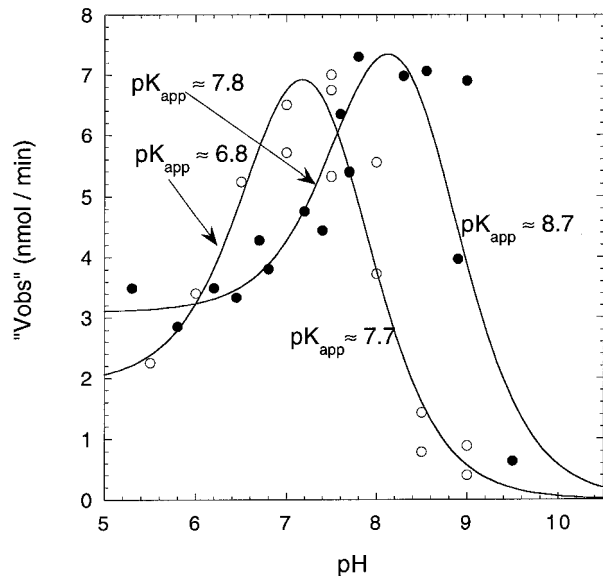


**Fig. 6** pH Dependence of the Activity of P14G-LH (○) and Comparison with wt-LH (●).

Conditions: [FAD] and [NADPH] = 300  $\mu\text{M}$ , [L-lysine] = 1.5 mM in buffers: MES,  $\text{KPi}$ , Tris and Tricine at an ionic strength of 0.1 M. The (●) data points were taken from (Macheroux *et al.*, 1993). The fits to the data points were obtained using appropriate 'pH equations', for two ionizations (see Materials and Methods for details). 'V\_obs' at pH < 5 were 3.1 (nmol/min) and 2.1 (nmol/min) for wt-LH (●) and P14G-LH (○), respectively. Note that the pK's derived from the plots are apparent ones.

essentially the same for the wild-type and mutant enzyme. Most importantly the shape of the pH-dependence is retained; however that of P14G-LH is shifted to a lower pH-value by approximately 1 unit. The two bell-shaped profiles also reflect two apparent pK's at 6.8 and 7.7 for P14G-LH, and 7.8 and 8.7 for the wild-type enzyme. These pK's have not been recognized in the previous study with the wild-type enzyme (Macheroux *et al.*, 1993). To which extent they reflect intrinsic ionizations of functional groups at the active center of the enzyme cannot be deduced from the present data. In general, such pH profiles of enzymatic activities include also the contributions of pH dependent kinetic terms (Dixon and Webb, 1979).

## Discussion

In the course of constructing the P14G mutant we sequenced the whole *aerA* gene and found differences to the published sequence (Herrero *et al.*, 1988). These differences may be due to the fact that the genes, originally cloned from different plasmids (pCoIV-K30 and pCoIV-K311, respectively) are indeed different or that one of the sequence determinations was incorrect. The observed differences on the DNA level (Table 1), which could be reproduced in two independent complete sequence determinations, are reflected by a different content of cysteine residues: The sequence published earlier by Herrero *et al.* (1988) predicts six cysteines whereas our sequence pre-

dicts only five. The results from DTNB titrations confirm the presence of five cysteine residues. Therefore we conclude that the sequence published by Herrero *et al.* (1988) is incorrect. This is also corroborated by the results of a recent publication (Marrone *et al.*, 1997) which shows that the sequence of *iucD* from pColV-K30 is identical to our sequence.

The putative FAD binding site of lysine N<sup>6</sup>-hydroxylase and other hydroxylases involved in siderophore biosynthesis consists of a GxGxGP motif in the N-terminal part of the protein (Stehr *et al.*, 1998). The unusual proline in this sequence prompted us to investigate the role of this residue in determining the affinity for FAD and its possible influence on catalysis. Since the typical nucleotide binding fold features a glycine instead of a proline, replacement of the proline by glycine can be regarded as an attempt to restore such a typical fold. As demonstrated by the kinetic analysis of the enzymatic properties of P14G-LH, this amino acid exchange has produced an enzyme with altered  $K_m$  values for FAD, NADPH and L-lysine.

The largest effect is observed for FAD, the  $K_m$  value of which is increased considerably from 2  $\mu\text{M}$  to  $\approx 400 \mu\text{M}$ . In addition, higher concentrations of both FAD and NADPH appear to induce inhibition, as is also the case with wt-LH. This suggests that each 'nucleotide' can bind two-fold to the active site of P14G-LH, which is probably due to the similarity of their adenosine moieties. Occupation of the binding pocket of the 'second nucleotide' will thus result in inhibition.

The most intriguing conclusion, however, can be derived from Figure 6. It is apparent that the maximal activities are comparable, as are the activity vs. pH profiles of wt-LH and of P14G-LH, the profile of the second being shifted by one unit toward lower pH. This indicates that the basic catalytic machinery of P14G-LH is intact.

On the other hand, although the catalytic activity of the enzyme with respect to the NADPH-oxidation rate is unaffected by the proline to glycine exchange, a higher degree of uncoupling, i.e. much less substrate hydroxylation per oxidized NADPH, is observed with P14G-LH. This indicates that, in P14G-LH, the interaction of NADPH and FAD is not affected as much as the next step in the catalytic sequence, i.e. the reaction of the FAD-4a-hydroperoxide with the N-terminal amino function of the substrate molecule.

The increase in  $K_m$  values can safely be interpreted as resulting from weaker binding of the reaction partners. This and the pK shifts are likely to result from a more open conformation of P14G-LH and/or increased access of solvent to the active site, which results in a different dielectric environment for the involved functional groups. In any case, the effects observed with P14G-LH clearly demonstrate the importance of the N-terminal part of the protein for its catalytic properties. This questions the interpretations by Viswanatha and coworkers who have found relevant activity for an N-terminally truncated, recombinant lysine N<sup>6</sup>-hydroxylase (Thariath *et al.*, 1993). At first sight, the latter finding could be interpreted in terms of a non-in-

volvement of the N-terminus in FAD-binding. However, close inspection of the 3D structure of para-hydroxybenzoate hydroxylase and phenol hydroxylase, two monooxygenases belonging to the same family, reveals that the FAD-cofactor is bound in an elongated form with various hydrogen bond interactions between amino acids and the isoalloxazine, ribityl and adenine moieties (Wierenga, 1979; Enroth *et al.*, 1998). Although the N-termini in these two proteins are involved in FAD-binding, as proposed also for lysine N<sup>6</sup>-hydroxylase (Stehr *et al.*, 1998), the majority of interactions occurs with central and even C-terminal parts of the protein. Since the relative contributions of these interactions for FAD binding are not yet known, it is conceivable that deletion of the N-terminus in lysine N<sup>6</sup>-hydroxylase does not lead to a complete loss of FAD binding and thus activity might be retained by the truncated protein. On the other hand, the adverse effect of the P14G mutation on FAD binding and the pH-activity profile clearly indicates the involvement of the N-terminus in maintaining the structural and catalytic integrity of the protein.

A multiple sequence alignment of four N-hydroxylating enzymes with glucose oxidase, glutathione reductase, *p*-hydroxybenzoate hydroxylase and phenol hydroxylase shows homology in the assumed FAD binding box (Figure 7). In contrast to the alignment with flavin monooxygenases (Stehr *et al.*, 1988) the Gly-X-Gly-X-X-Gly motif of the latter four enzymes aligns with the Gly-X-Gly-Pro-X-Asn/His motif of the N-hydroxylating enzymes. Compared to the alignment with FMO's the sequences of the N-hydroxylating enzymes are shifted by two residues. This could explain why the strong binding of FAD to lysine hydroxylase could not be restored by the P14G mutation

<i>iucD</i>	DFIGVGTGPFNLSIAALSHQ	25	sp:P11295
<i>alcA</i>	DFVAIGIGPFNLSLALSAP	26	p: JC4556
<i>pvdA</i>	DLIGVGFGRSNIALAIALQE	31	p: A49892
<i>sid1</i>	DLIGIGFGRSIALALSISLRE	57	p: A47266
GOD	DYIIAGGGLTGLTTAARLTE	40	sp:P13006
GRS	DYLVIGGSGGLASARRAAE	41	sp:P00390
PHBH	QVAIIIGAGE SGLLLGQLLHK	23	sp:P15245
PHHY	DVLIVGAGEAGLMAARVLSE	28	sp:P00438
	GxGxxG		

**Fig. 7** Multiple Sequence Alignment of 8 FAD-Binding Proteins. The sequences were aligned using the program MACAW (Schuler *et al.*, 1991). First column: protein names; last column: accession numbers from SWISS-PROT (sp) and PIR (p) databases; the number after the sequence shows the position of the last residue in their respective sequence. The consensus sequence is shown in the bottom row. Residues that are conserved in more than 80% of the sequences are shaded in grey. The proline residue that is common to all four N-hydroxylating enzymes is shaded in dark grey.

Aligned sequences: *incD* – L-lysine N<sup>6</sup>-hydroxylase (*Escherichia coli*); *alcA* – alcaligin biosynthesis enzyme (*Bordetella bronchiseptica*); *pvdA* – L-ornithine N<sup>5</sup>-oxygenase (*Pseudomonas aeruginosa*); *sid1* – L-ornithine N<sup>5</sup>-oxygenase (*Ustilago maydis*); GOD – glucose oxidase (*Aspergillus niger*); GRS – glutathione reductase (human erythrocytes); PHBH – *p*-hydroxybenzoate hydroxylase (*Pseudomonas fluorescens*); PHHY – phenol hydroxylase (*Trichosporon cutaneum*).

suggesting an N16G mutation as a target for further investigation.

The work reported in this paper was greatly facilitated by the fact that we had previously developed a new expression system for the enzyme by cloning the *aerA* gene from *fur*-regulated pRG111 into IPTG inducible pQE30 (Hermes *et al.*, 1994). In pQE30 *aerA* contains a 6xHis affinity tag coding sequence and the expression is under the control of the *E. coli* phage T7 promoter combined with two *lac* operator sequences. While the total activity in the cell extract from 10 g of cells (wet weight) was 5.4 U (spec. act. 0.011 U/mg) after dialysis when the gene was under iron control (Plattner *et al.*, 1989), the activity after cell disruption and dialysis was about 25 U (spec. act. 0.083 U/mg) after induction of the fusion protein with IPTG. Using the published method for enzyme purification (Plattner *et al.*, 1989) the yield was about 25% compared to 84% when the enzyme was purified by a single-step adsorption/elution from the Ni-NTA resin, and even the specific activity of the purified enzyme was greatly increased (to 0.46 U/mg). The resin adsorption was indispensable when clones were selected after site-directed mutagenesis. Due to the tremendous decrease of cofactor affinity no enzyme activity was found using the conventional resting cell assay, but concentration of the expressed protein by Ni-NTA adsorption allowed to identify clones expressing His-tag fusion P14G lysine hydroxylase. It is quite remarkable that the overexpression of the His-tag LH yields a fully soluble enzyme while P14G-LH was obtained – under identical conditions of expression – as inclusion bodies which can only be solubilized in 6 M urea.

Finally, the retaining of maximal activity and the overall activity/pH profile is a case in point to demonstrate the necessity to carefully characterize a mutant protein, at least with respect to specific parameters, as opposed to simply compare activities under a single set of parameters which are optimal for a wild-type enzyme.

## Materials and Methods

### Bacterial Strains, Plasmids and Culture Conditions

*Escherichia coli* EN222 harbouring pRG111 has been described previously (Gross *et al.*, 1984; Plattner *et al.* 1989). *Escherichia coli* M15 harbouring pREP4 (Qiagen, Hilden, Germany) was used as host for pQE30 (Qiagen), pMR30 and pMS30.

### Cloning of *aerA*

Cloning of *aerA* was accomplished as described in Figure 1A. *aerA* from pRG111 of *Escherichia coli* EN222 was amplified by PCR. Via the PCR primers an additional His-tag, enterokinase cleaving site and *Bam*HI and *Pst*II restriction sites sequences were introduced. The fragment was ligated into the *Bam*HI – *Pst*II site on the expression vector pQE30 (yielding pMR30) and used to transform *E. coli* strain M15. Transformants were selected on LB agar containing kanamycin (25 µg/ml) and ampicillin (100 µg/ml). Transformation of *E. coli* was done by electroporation (Electro Cell Manipulator ECM 600; BTX Inc., San Diego, USA) according to the manufacturers instructions. One transformant with high ly-

sine N<sup>6</sup>-hydroxylase activity was selected and designated *E. coli* M15-0 (Hermes *et al.*, 1994).

### Growth Conditions

*Escherichia coli* M15-0 was grown on a rotary shaker at 37 °C in LB medium (Miller, 1972) supplemented with ampicillin (100 µg/ml) or ampicillin plus kanamycin (25 µg/ml). For the enzyme preparation cells were grown in a New Brunswick MF-14 fermenter (New Brunswick Scientific Co., New Jersey, USA) filled with 10 l of LB medium containing appropriate concentration of antibiotic(s). At OD<sub>578</sub> = 2.0 IPTG was added to a final concentration of 1 mM. During fermentation the activity of lysine N<sup>6</sup>-hydroxylase was measured by the resting cell assay. Cells were harvested at OD<sub>578</sub> = 4–5 by centrifugation and were stored at –20 °C.

*E. coli* M15-2 was grown as described above, but at 30 °C and a final IPTG concentration of 0.1 mM was used, added at an OD<sub>578</sub> = 1.0. Cells were harvested 90 minutes after induction with IPTG and stored frozen in 5 g portions.

### Construction of the PMS30 by Site-Directed Mutagenesis

The plasmid pMR30 containing *aerA* (see above) was used as a template for the polymerase chain reaction (PCR). Primers for introducing mutation by PCR were

5'-GC GGA TCC GAT GAC GAT GAC AAA ATG AAA AAA AGT GTC GAT TTT ATT GGT GTA GGG ACA GGG **GGT** TTT AAT CTC AGC-3' (forward) and  
5'-GG CTG CAG CTA GGT GCC GCT GCG CCA C-3' (reverse)

(the mismatched bases are in bold type). PCR with forward and reverse primers generated a 1.3 kb DNA fragment. For PCR with different-length primers the following PCR program was designed: one cycle taking 1 min to reach 95 °C and 2 min at 95 °C (melting) and further 25 cycles each taking 23 s to reach 95 °C, 30 s 95 °C (melting), 40 s to reach 55 °C and 30 s at 55 °C (primer annealing), 17 s to reach 72 °C and 60 s at 72 °C (extension). The PCR product was purified by agarose gel electrophoresis (QI-Aquick Gel Extraction Kit) and digested with *Bam*HI and *Pst*II. The mutated fragment was cloned into pQE30. The plasmid carrying the mutated *aerA* gene was used to transform *E. coli* strain M15. Transformants were selected on LB agar containing kanamycin (25 µg/ml) and ampicillin (100 µg/ml) and transformants producing LH were selected by a nickel-chelate chromatography-assay (Qiagen). The proteins were visualized by Coomassie Brilliant Blue staining on 12% polyacrylamide gels. Several transformants producing mutated LH were selected and the CCA →GGT substitution and identity with the template DNA was confirmed by DNA sequencing. Sequencing of *aerA* and [P14G]*aerA* was done with the following forward primers:

5'-TAGGCGTATCACGAGGCCCT-3',  
5'-AACTATCTGGTGAAGCACAAAAGT-3',  
5'-TTACGCGGGGAATGGGAGA-3',  
5'-ACGTCGATTGTTTCTGGTGC-3'

and reverse primers:

3'-TAGAGTCGTAACGACGCAA-  
5',3'-GGACAACTATCTAGGTCATTAC-5'.

The sequencing reactions were performed using a Dye-Terminator Cycle Sequencing Kit in a PCR machine (Perkin Elmer Gene Amp PCR system 9600). The DNA sequence determination was done with an automatic DNA Sequencer (Applied Biosystems Model 373A). One transformant, showing identical sequence with the template DNA, only carrying the CCA →GGT substitution was selected and designated *E. coli* M15-2. The plasmid carrying the

[P14G]*aerA* gene was named pMS30. The mutated enzyme was referred to as P14G lysine hydroxylase. The nucleotide sequence of *aerA* and [P14G]*aerA* from pColV-K311 were deposited under the GenBank accession numbers AF016586 and AF016587, respectively.

#### Purification of wt-Lysine N<sup>6</sup>-Hydroxylase

With some modifications the wt-LH was purified by ammonium sulfate precipitation, Superdex gel- and ion-exchange chromatography as described previously for the wild-type enzyme (Plattner *et al.*, 1989). Before dialysis the crude extract was treated for 45 min with RNase and DNase (10 µg/ml, 40 µg/ml) with addition of a final concentration of 40 mM MgSO<sub>4</sub>. To the buffers for performing the separation on MonoQ and Ni-NTA affinity chromatography no dithiothreitol was added. Finally, affinity chromatography using Ni-NTA resin was performed. The Ni-NTA column was prepared to the manufacturers protocol (Qiagen, Hilden, Germany) and pre-equilibrated with 50 mM Tris/HCl, 300 mM KCl, 50 mM imidazole (pH 7.5) and 10% glycerine. The LH was eluted by a gradient of imidazole (50–350 mM). The purity of the protein was examined by sodium dodecyl sulfate polyacrylamide gel electrophoresis (SDS-PAGE; Laemmli and Favre, 1973), and proteins were visualized with Coomassie Brilliant Blue or silver staining (Blum *et al.*, 1988).

#### Purification of P14G Lysine N<sup>6</sup>-Hydroxylase

Purification was done by direct Ni-NTA affinity chromatography. Two ml buffer (50 mM Tris/HCl pH 7.5 containing 300 mM KCl and 10% glycerol) were added to 1 g of frozen cells each. After thawing 10-ml portions were sonicated as described before (Plattner *et al.*, 1989). After DNase/RNase treatment an aliquot of the supernatant containing 75–100 mg protein was loaded directly onto a Ni-NTA column, prepared as described above. After washing with 10 ml 10 mM imidazole, P14G lysine hydroxylase was eluted by a gradient of imidazole (50–350 mM). As in the case of wild-type lysine N<sup>6</sup>-hydroxylase, preparations of the P14G mutant were essentially free of FAD, and there is no indication of tight binding of the cofactor, e.g. when analyzed spectrophotometrically. The purity of the mutant protein and the correct molecular mass are documented by the SDS gel electrophoresis shown in Figure 2.

#### Enzyme Assays

Enzyme activity was assayed by measuring the production of N-hydroxy-lysine in the iodine oxidation assay (Plattner *et al.*, 1989) or with the NADPH-oxidation assay (Macheroux *et al.*, 1993).

The iodine oxidation assay was carried out in 0.1 M potassium phosphate, pH 7, containing NADPH (500 µM), L-lysine (1.5 mM) and FAD (5 µM for the wild-type enzyme and 300 µM FAD for the P14G mutant enzyme). The enzyme concentrations were: 0.2 µM for wt-LH and 1–2 µM for P14G-LH, in a volume of 1 ml. Upon mixing the reactants, the mixture was incubated at 37 °C for 30 min (wild-type LH) or 1 h (P14G mutant). The reaction was stopped by addition of 0.5 ml 0.2 N perchloric acid. In the iodine oxidation test (Tomlinson *et al.*, 1971; Gross *et al.*, 1984) 1 ml of the supernatant was incubated with 0.5 ml 1% sulfanilic acid in 25% glacial acetic acid and 0.2 ml 1.3% iodine in glacial acetic acid for 5 min at room temperature. Upon this treatment, excess iodine was destroyed with 0.2 ml 0.1 N sodium thiosulfate. Finally, 0.2 ml of 0.6% α-naphthylamine in 30% glacial acetic acid was added which leads to the formation of a pink color. After 30 min incubation the concentration of the dye was measured spectrophotometrically at 520 nm ( $\epsilon \approx 17000 \text{ M}^{-1} \text{ cm}^{-1}$ ).

The NADPH-oxidation assay was carried out in 0.1 M Tris, pH 8, containing NADPH (300 µM), L-lysine (1.5 mM) and FAD (10 µM

for wild-type and 300 µM for the P14G mutant) at 25 °C. The concentration of wt-LH and P14G mutant in the assay was 0.5 µM. Enzyme activity was estimated from the decrease of NADPH absorbance at 340 nm ( $\epsilon \approx 6300 \text{ M}^{-1} \text{ cm}^{-1}$ ): one unit of activity represent the µmols of NADPH consumed per minute.

Expression of the wild-type enzyme was measured *in vivo* by a resting cell experiment as follows: 9 ml of an IPTG-induced culture were centrifuged, washed with saline and resuspended in a solution containing 10 mM L-lysine and 5 g/l glucose. After incubation for 30 min on a rotary shaker at 37 °C 1 ml of the culture was used for the iodine oxidation test (Plattner *et al.*, 1989). Expression of the P14G enzyme was measured by Ni-NTA in crude extract after sonication (Plattner *et al.*, 1989) and by nickel-chelate chromatography-assay (Qiagen).

#### Miscellaneous Methods

Activity measurements based on absorbance changes of substrate/product were measured with a Kontron Uvikon 810 or 930 photometer. This instrument is fairly linear up to an absorbance of  $\approx 2.4$ . At absorbance values  $> 2$  OD units cuvetts with an optical path of 4 mm were employed. For all data reported in this work the two methods yielded similar values. The plots of the data in the various Figures were produced using KaleidaGraph<sup>®</sup>. The fits to the data points were obtained using either standard algorithms or, in the case of substrate inhibition with the equation  $y = (x \cdot V_{\max}) / (K_1 + x + [(x^2)/K_i])$  (Fersht, 1977, pp. 98, equation 3.51) where  $y$  = observed activity,  $x$  = [substrate],  $V_{\max}$  = maximal activity,  $K_1$  =  $K_m$  for substrate variable, and  $K_i$  is the inhibition constant for the same substrate. The algorithms used to generate the fits in Figure 6 were adapted from the equations described by Dixon and Webb (1979, pp. 138–164).

#### Acknowledgements

We thank Prof. V. Braun, Tübingen, for critical discussion, Dr. H. Plattner for valuable help and A. Janczikowski for technical assistance. This work was supported by grants of the Deutsche Forschungsgemeinschaft to S.G. and H.D.

#### References

- Blum, H., Beier, H., and Gross, H.J. (1988). Improved silver staining of plant proteins, RNA and DNA in polyacrylamide gels. *Electrophoresis* 8, 93–99.
- Braun, V. (1981). *Escherichia coli* containing the plasmid Col V produce the iron ionophore aerobactin. *FEMS Microbiol. Lett.* 11, 215–228.
- De Lorenzo, V., Bindereif, A., Paw, B.H., and Neilands, J.B. (1986). Aerobactin biosynthesis and transport genes of plasmid ColV-K30 in *Escherichia coli* K-12. *J. Bacteriol.* 165, 570–578.
- Dixon, M., and Webb, E.C. (1979). *Enzymes*, 3<sup>rd</sup> ed. (New York: Academic Press, Longman Lt.), pp. 138–164.
- Engelbrecht, F., and Braun, V. (1986). Inhibition of microbial growth by interference with siderophore biosynthesis. Oxidation of primary amino groups in aerobactin synthesis by *Escherichia coli*. *FEMS Microbiol. Lett.* 33, 223–227.
- Enroth, C., Neujahr, H., Schneider, G., and Lindqvist, Y. (1998). The crystal structure of phenol hydroxylase in complex with FAD and phenol provides evidence for a concerted conformational change in the enzyme and its cofactor during catalysis. *Structure* 6(5), 605–617.

- Fersht, A. (1977). Enzyme structure and mechanism. (New York: W.H. Freeman and Company), pp. 93–101, 137–143.
- Gross, R., Engelbrecht, F., and Braun, V. (1984). Genetic and biochemical characterization of the aerobactin synthesis operon on pColV. *Mol. Gen. Genet.* 196, 74–80.
- Gross, R., Engelbrecht, F., and Braun, V. (1985). Identification of the genes and their polypeptide products responsible for aerobactin synthesis by pColV plasmids. *Mol. Gen. Genet.* 207, 204–212.
- Hermes, M., Mayerbacher, H.J., Plattner, H., and Diekmann, H. (1994). A new bacterial strain for lysine-N<sup>6</sup>-hydroxylase. *Bioengineering (Graefelf) 10* (special issue 3), 112.
- Herrero, M., De Lorenzo, V., and Neilands, J.B. (1988). Nucleotide sequence of the *iucD* gene of the pColV-K30 aerobactin operon and topology of its product studied with *phoA* and *lacZ* gene fusions. *J. Bacteriol.* 170, 56–64.
- Laemmli, U.K., and Favre, M. (1973). Maturation of the head of bacteriophage T4. *J. Mol. Biol.* 80, 575–599.
- Macheroux, P., Plattner, H.J., Romaguera, A., and Diekmann, H. (1993). FAD and substrate analogs as probes for lysine N<sup>6</sup>-hydroxylase from *Escherichia coli* EN 222. *Eur. J. Biochem.* 213, 995–1002.
- Marrone, L., and Viswanatha, T. (1997). Effect of selective cysteine → alanine replacements on the catalytic functions of lysine: N<sup>6</sup>-hydroxylase. *Biochim. Biophys. Acta* 1343(2), 263–277.
- Miller, J.H. (1972). *Experiments in Molecular Genetics*. (Cold Spring Harbor, New York: Cold Spring Harbor Laboratory Press).
- Plattner, H., Pfefferle, P., Romaguera, A., Waschütza, S., and Diekmann, H. (1989). Isolation and some properties of lysine N<sup>6</sup>-hydroxylase from *Escherichia coli* strain EN222. *Biol. Metals* 2, 1–5.
- Schuler, G.D., Altschul, S.F., and Lipman, D.J. (1991). A workbench for multiple alignment construction and analysis. *Proteins* 9(3), 180–190.
- Stehr, M., Diekmann, H., Smau, L., Seth, O., Ghisla, S., Singh, M., and Macheroux, P. (1998). A hydrophobic sequence motif common to N-hydroxylating enzymes. *Trends Biochem. Sci.* 23, 56–57.
- Thariath, A.M., Fatum, K.L., Valvano, M.A., and Viswanatha, T. (1993). Physico-chemical characterization of a recombinant cytoplasmatic form of lysine N<sup>6</sup>-hydroxylase. *Biochim. Biophys. Acta* 1203, 27–35.
- Tomlinson, G., Cruickshank, W.H., and Viswanatha, T. (1971). Sensitivity of substituted hydroxylamines to determination by iodine oxidation. *Anal. Biochem.* 44, 670–679.
- Weinberg, E.D. (1984). Iron withholding: a defense against infection and neoplasia. *Physiol. Rev.* 64, 65–102.
- Wierenga, R.K., De Jong, R.J., Kalk, K.H., Hol, W.G.J., and Drenth, J. (1979). Crystal structure of p-hydroxybenzoate hydroxylase. *J. Mol. Biol.* 131, 55–73.
- Wierenga, R.K., De Maeyer, C.H., and Hol, W.G.J. (1985). Interaction of pyrophosphate moieties with  $\alpha$ -helices in dinucleotide binding proteins. *Biochemistry* 24, 1346–1357.

*Received April 20, 1998; accepted November 4, 1998*